



**First Principles Calculations for Photovoltaic and
Optoelectronic Properties of Pristine and Doped-Graphene**

by

**Agbolade Lukman Olatomiwa
(2131913587)**

A thesis submitted in fulfillment of the requirements for the degree of
Master of Science

**Institute of Nano Electronic Engineering
UNIVERSITI MALAYSIA PERLIS**

2024

PERMISSION TO USE

In presenting this thesis in fulfilment of the requirements for a postgraduate degree from Universiti Malaysia Perlis (UniMAP), I agree that permission for the copying of this thesis in any manner, in whole or in part, for scholarly purpose may be granted by the Director of the Centre for Graduate Studies. It is understood that any copying or publication or use of this thesis or parts thereof for financial gain shall not be allowed without my written permission. It is also understood that due recognition shall be given to me and to Universiti Malaysia Perlis (UniMAP) for any scholarly use which may be made of any material from my thesis.

Requests for permission to copy or to make other use of materials in this thesis, in whole or in part, should be addressed to:

Director, Centre for Graduate Studies
Administration Block, 1st Floor,
Engineering Training Center Building,
Pauh Putra Campus, 02600 Arau Perlis
Tel : +604-9885712 Fax : +604-9885740,
e-mail : cgs@unimap.edu.my

ACKNOWLEDGEMENT

My deepest gratitude goes to my supervisors, Dr. Tijjani Adam and Prof. Ts. Dr. Uda, for their support, thought-provoking suggestions, and counsel throughout this program. I would also like to thank Dr. Nur Hamidah binti Abdul Halim, the former programme chairperson at the Institute of Nano Electronic Engineering, and the entire staff of the Institute of Nano Electronic Engineering and the Faculty of Engineering Technology for providing a conducive environment for my research.

I appreciate the efforts of Prof. Abdullah Chik, Prof. Y.K. Sanusi, Dr. Akeem Adewale, Dr. Joshua Majekodunmi, and Dr. Collins Okon Edet for their useful discussions and contributions to the successful completion of this research. This work would certainly be lifeless without their colourful input. In addition, I appreciate the Malaysian Ministry of Higher Education for funding my program.

Lastly, I would like to take this chance to thank my family, relatives, and friends for their understanding sacrifices throughout the course of the program.

©This item is protected by original copyright

TABLE OF CONTENTS

	PAGE
DECLARATION OF THESIS	i
PERMISSION TO USE	ii
ACKNOWLEDGEMENT	iii
TABLE OF CONTENTS	iv
LIST OF TABLES	viii
LIST OF FIGURES	ix
LIST OF ABBREVIATIONS	xiii
LIST OF SYMBOLS	xiv
ABSTRAK	xv
ABSTRACT	xvi
CHAPTER 1 : INTRODUCTION	1
1.1 Research Background	1
1.2 Problem Statement	3
1.3 Objectives of the Research	5
1.4 Research Scope	6
1.5 Limitations	7
CHAPTER 2 : LITERATURE REVIEW	8
2.1 Introduction	8
2.2 Overview of the Heritage of Graphene and Selected Properties	9
2.3 The Structural Properties of Pure Graphene Material	11

2.4	The Electronic Properties of Pure Graphene	13
2.5	The Optical Properties of Pure Graphene of Material	16
2.6	Modification of the Electronic and Optical Properties of Graphene by Chemical Doping	19
2.7	Overview of Density Functional Theory Models Employed for Optoelectronic Properties of Graphene	31
2.7.1	The Schrodinger Equation	33
2.8	Hohenberg and Kohn Theorems	35
2.8.1	Kohn-Sham Theory	37
2.9	Exchange-Correlation Functional	39
2.9.1	Local Density Approximation	39
2.9.2	Generalized Gradient Approximation (GGA)	40
2.9.3	Basis Sets	42
2.10	Pseudopotential Approach	42
2.11	First Principles Calculations on CASTEP Code	44
2.12	Mulliken Charge Population Analysis	45
CHAPTER 3 : METHODODOLOGY		47
3.1	Introduction	47
3.2	The Overall flow Chart.	48
3.3	Determining the Structural Properties of Pure Graphene	50
3.3.1	The Atomic Unit Cell of Graphene	51
3.3.2	Generating of Supercell Structures of Pure Graphene	52
3.3.3	Modelling of Boron and Beryllium-Doped Graphene	53
3.3.4	K-point and Cut-off Energy Convergence Tests	56
3.3.5	Geometry Optimisation	57
3.3.6	SCF Calculation	58
3.3.7	Single Point Calculation	59

3.4	Determining the Electronic and Optical Properties	59
3.4.1	Band Structure Calculation	60
3.4.2	Calculation of the Energy Band Gap	61
3.4.3	Density of State Calculation	61
3.4.4	Determining of the Optical Properties	62
CHAPTER 4 :	RESULTS	63
4.1	Introduction	63
4.2	The Structural Properties of Pure Graphene	63
4.2.1	The Supercell of Pure Graphene	64
4.3	The Electronic and Optical Properties of Pure Graphene	65
4.3.1	Study of the Band Structure of Pure Graphene	65
4.3.1.1	Study of the Density of State of Pure Graphene	66
4.3.2	Dielectric Function Analysis of Pure Graphene	68
4.3.2.1	Absorption Coefficient Analysis of Pure Graphene	69
4.3.2.2	Complex Refractive Index of Pure Graphene	71
4.4	The Structural Properties of Doped Graphene Supercell	73
4.4.1	The Boron and Beryllium-Doped Graphene Models	73
4.4.2	Mulliken Charge Analysis	76
4.5	The Electronic and Optical Properties of Doped-Graphene	80
4.5.1	Study of the Band Structure of Boron and Beryllium-Doped Graphene	80
4.5.1.1	Study of Density of State of Boron and Beryllium-Doped Graphene	82
4.5.1.2	Study of Dielectrics of Boron and Beryllium-Doped Graphene	91
4.5.2	Absorption Coefficient Analysis of Boron and Beryllium-Doped Graphene	94

4.5.2.1	Complex Refractive Index of Boron and Beryllium-Doped Graphene	98
CHAPTER 5 :	CONCLUSION AND RECOMMENDATIONS	99
5.1	Conclusion	99
5.2	Recommendations and Future Outlook	101
	REFERENCES	102
	LIST OF PUBLICATIONS	123

©This item is protected by original copyright

LIST OF TABLES

		PAGE
Table 2.1	The calculated parameters for pure and different doped graphene	19
Table 2.2	The prospects and gaps observed for different doped graphene systems	23
Table 2.3	Single and co-doped graphene systems, applications, and gaps	25
Table 2.4	Pure and singly doped graphene systems, applications, and gaps	29
Table 2.5	Dual-doped graphene systems, applications, and gaps	30
Table 3.1	The parameters employed during the geometry optimisation.	58
Table 3.2	The special symmetry points of the irreducible wedge of the first Brillouin zone of graphene	61
Table 4.1	The lattice parameters before and after optimisation, cell volume and bond lengths of pure graphene.	65
Table 4.2	The lattice parameters and percentage difference of boron and beryllium doped graphene models	74
Table 4.3	The optimised bond length of boron and beryllium doped graphene models	75
Table 4.4	The listed highlights the Mulliken charge populations of pure, B and Be-doped graphene.	78
Table 4.5	The calculated band gap, measured using XMGrace, and the bond length of boron and beryllium doped graphene compared with different studies	82

LIST OF FIGURES

	PAGE	
Figure 1.1	The schematic illustration shows the two carbon atoms in the unit cells of graphene with its Bravais lattices, and the primitive vectors	2
Figure 2.1	Graphene's global related publication from 2004 till 2021 and graphene research publication per year from 2010 – 2021 (Madsuha et al., 2022).	9
Figure 2.2	The schematic illustration of the origin and the graphite transformation to graphene's atomic structure. The transformation process shows that graphene, a 2D basic unit of carbon can be stacked into (C) 3-D graphite (D) rolled into 1-D nanotubes (E), and folded into 0-D fullerene (Geim & Novoselov, 2009).	13
Figure 2.3	(a-c) Schematic illustration of the formation process from the basic element of graphene bonding properties and (d) the SEM image of mono-layer graphene (e-f) The honeycomb lattice and its Brillouin zones (f) the band structure of pure graphene. The Left-hand side (L.H.S) reveals the interpenetrating triangular lattices that make up the lattice structure of 2D graphene. The right-hand side (R.H.S) reveals the Dirac Cone which is created by the valence and conduction band crossing at the K and K' point (Castro Neto et al., 2009.; Jia et al., 2016). This is indicated in (f) the calculated band structure of Pure graphene (Feher et al., 2011.; Hosen et al., 2019).	14
Figure 2.4	(a) Schematic illustration of the energy bands near the Fermi level in graphene. The horizontal plane in the first Brillouin zone of graphene. The conduction and valence band meets at the K and K' points in the Dirac cone (b) The Conic energy	

	bands near the K and K' points (c) The density of states with the fermi energy near the Fermi level (Garg et al., 2014).	16
Figure 2.5	The optimised geometry and the electronic band structure of Nitrogen-doped graphene. The Nitrogen atom is symbolised by the red ball and the bond lengths indicated in the rings are measured in Å (Rani & Jindal, 2013).	21
Figure 2.6	The reflectivity for pristine graphene (a) as compared with graphene dual doped of Boron and Nitrogen in increasing order of concentrations of boron at different percentages (b) 12.75 (c) 18.75 (d) and 37.5 (e) and 75 percent respectively for perpendicular and parallel polarisation. Figure remodified from Ref (Rani et al., 2014).	28
Figure 2.7	The graphical illustration of the real potential (dashed line) and pseudopotential (solid line) and their corresponding wave functions.	44
Figure 3.1	The overall flowchart of the stages and properties of graphene observed.	50
Figure 3.2	The unit cell of pure graphene is displayed with black lines and the compasses on the side of the visuals show the direction of the translation vectors. The brown atoms represent the carbon atoms of graphene	52
Figure 3.3	The supercell structure of pure graphene	53
Figure 3.4	Introduction of single, dual and tri-doped Boron (B) and Beryllium (Be) atoms in graphene	55
Figure 3.5	The convergence of total energy with k-points for pure and doped graphene	57
Figure 3.6	Flow Chart of SCF calculation	59

Figure 3.7	Schematic illustration of the high symmetry path in the hexagonal Brillouin zone and the reciprocal lattice vectors (Cuono et al., 2018; Karmakar et al., 2021).	60
Figure 4.1	The lattice structures of the optimised pure graphene supercell (a) frontal view (b) the top view (c) the bottom view. The brown circle indicates the carbon atoms in the graphene lattice.	64
Figure 4.2	The calculated band structure of pure graphene along the high symmetry points in the Brillouin zones	66
Figure 4.3	(a) Total density of states of pure graphene (b) Partial density of states of pure graphene showing the contributions of carbon 2s and 2p orbitals.	67
Figure 4.4	The dielectric function shows the real and the imaginary parts of pure graphene. The inset details the optical dielectric function in the IR, visible and UV regions.	69
Figure 4.5	(a) The absorption coefficient and (b) the refractive index of pure graphene. The inset shows the details of the optical absorption and refractive index in the infrared, visible, and ultraviolet regions.	70
Figure 4.6	The frontal views of the optimized lattice of (a) boron (a1) Single doped (a2) Dual doped (a3) Tri doped and (b) beryllium (b1) Single doped, (b2) Dual doped and (b3) Tri-doped graphene supercell via the ab initio framework.	79
Figure 4.7	The band structure of boron (a) single-doped (b) dual-doped (c) tri-doped and beryllium (d) single-doped (e) dual-doped (f) Tri-doped graphene calculated using the PBE technique along the high symmetry point. The results indicate the created band gaps, with the band lines showing the transition of electrons from the valence band to the conduction bands.	81

- Figure 4.8 Boron-single, dual, and tri-doped configurations showing C2p and B2p contributions (a, d, g) Total density of states (b, e & h) Partial density of states showing C 2p and C 2s contributions and (c, f & i) Partial density of states showing B 2p and 2s orbitals. 87
- Figure 4.9 Beryllium-single, dual, and tri-doped configurations showing C2p and B2p contributions (a, d, g) Total density of states (b, e & h) Partial density of states showing C 2p and C 2s contributions and (c, f & i) Partial density of states showing B 2p and 2s orbitals. 90
- Figure 4.10 presents the dielectric function of doped graphene as follows: (a) real part and (b) imaginary parts for B-single-doped, dual-doped and tri-doped graphene (c) the real part and (d) imaginary parts for Be-single, dual and tri-doped graphene. Inset: gives details of the dielectric function in the infrared, visible and regions. 94
- Figure 4.11 shows the (a) absorption spectrum and (b) refractive index of B-single, dual and tri-doped (c) absorption coefficient and (d) refractive index of Be-single, dual and tri-doped graphene. The inset gives the optical absorption spectrum and refractive index in the IR, visible, and UV regions 97

LIST OF ABBREVIATIONS

<i>c</i>	Conduction Band
DFT	Density Functional Theory
DOS	Density of State
DSSCs	Dye-synthesized solar cells
E_G	Band gap energy
EELS	Electron energy loss spectroscopy
GGA	Generalized-gradient approximations
GO	Graphene oxide
GQDs	Graphene quantum dots
HF	Hartree-Fock
HREELS	High energy electron energy loss spectroscopy
IXS	Inelastic x-ray scattering
LDA	Local Density approximations
LO	Longitude optic
MC	Monte Carlo
MD	Molecular dynamics
N	Nitrogen
P	Primary value
PBE	Perdew, Becke, and Ernzerhof
PCE	Power Conversion Efficiency
<i>r</i>	Vector location
rGO	Reduced graphite oxide
SEM	Scanning electron Microscope
Sp^2	Trigonal hybridization
TEM	Transmission electron microscope
<i>u</i>	Vectors
<i>v</i>	Valence band
XC	Exchange-correlation
0D	Zero Dimensional
1D	One Dimensional
2D	Two dimensional
$1(\omega)$	Real parts of the complex dielectric function
$2(\omega)$	Imaginary parts of the complex dielectric function

LIST OF SYMBOLS

Å	Angstrom
B	Boron
Be	Beryllium
C	Carbon
CO	Carbon-monoxide
Fe	Iron
Ga	Gallium
\hat{H}	Hamiltonian
In	Indium
N	Nitrogen
O	Oxygen
P_x, P_y, P_z	Dumb-bell orbital
S Orbital	Spherical Orbital
Si	Silicon
Te	Tellurium
%	Percentage
π	Pi
σ	Sigma
Ψ	Wavefunction

©This item is protected by original copyright

Pengiraan Prinsip Pertama untuk Sifat-sifat Fotovolta dan Elektronik Optik bagi Grafen Asli dan Terdop

ABSTRAK

Kajian ini menggunakan pengiraan teori fungsi ketumpatan (DFT) dalam kod CASTEP untuk menyiasat kesan berubat bius boron (B) dan berilium (Be) ke atas sifat struktur dan optoelektronik grafen. Kaedah pengiraan melibatkan pengoptimuman geometri menggunakan algoritma (L-BFGS), fungsi penghampiran kecerunan umum (GGA) Perdew-Burke-Ernzerhof (PBE) dan fungsi pseudopotential ultrasoft. Analisis struktur mendedahkan populasi ikatan yang lebih tinggi dan kestabilan struktur yang dipertingkatkan dalam konfigurasi B-tela ubat bius berbanding sistem Be-ubat bius, dengan konfigurasi B-satu-ubat bius menunjukkan populasi bon tertinggi dan purata panjang bon terpendek. Sifat elektronik mendedahkan bahawa peningkatan kepekatan B-berubat bius membawa kepada jurang jalur yang lebih tinggi: B-tunggal (0.191 eV), B-dual (0.387 eV) dan B-tri (0.44 eV). Sebaliknya, konfigurasi Be-tela ubat bius mempamerkan jurang jalur yang lebih tinggi yang berkurangan dengan peningkatan berubat bius: Be-satu (0.60 eV), Be-dual (0.550 eV), dan Be-tiga-tela ubat bius (0.420 eV), mencadangkan potensi untuk pembawa yang dipertingkatkan. mobiliti. Analisis optik mendedahkan puncak penyerapan anjakan merah untuk grafen berubat bius B-tunggal, sesuai untuk optoelektronik inframerah, manakala kepekatan B-berubat bius yang lebih tinggi menyebabkan anjakan biru, membolehkan aplikasi kelihatan dan UV. Tela ubat bius Be-satu memaparkan puncak teranjak biru, manakala doped Be-dual mempamerkan penyerapan cahaya yang boleh dilihat dan Be-tiga-berubat bius telah memanjangkan puncak penyerapan di kawasan inframerah, menjadikannya sesuai untuk aplikasi UV dan penerima imej IR. Selain itu, grafen Be-tiga-tela ubat bius mempamerkan potensi tinggi untuk fotovoltaik, memaparkan berbilang puncak dalam julat yang boleh dilihat (1.6-2.4 eV), sekali gus memberikan sifat penyerapan yang lebih luas. Penemuan ini memberikan pandangan yang berharga untuk menyesuaikan sifat grafen melalui doping B dan Be terkawal untuk pelbagai aplikasi optoelektronik. Kajian menunjukkan bahawa berubat bius Be dan B boleh mendorong jurang jalur dalam grafen sehingga 0.60 eV dan 0.44 eV, masing-masing, memenuhi keperluan untuk transistor buka/tutup berasaskan grafen. Penyelidikan masa depan boleh meneroka pemodelan heterostruktur berasaskan grafen untuk optoelektronik generasi akan datang, memanfaatkan mobiliti cas tinggi dan struktur jalur boleh tala.

First principles Calculations for Photovoltaic and Optoelectronic Properties of Graphene

ABSTRACT

This study employed density functional theory (DFT) calculations within the CASTEP code to investigate the effects of boron (B) and beryllium (Be) doping on the structural and optoelectronic properties of graphene. The computational method involved geometry optimization using the (L-BFGS) algorithm, the Perdew-Burke-Ernzerhof (PBE) generalized gradient approximation (GGA) exchange-correlation functional, and ultrasoft pseudopotential. Structural analysis revealed higher bond populations and enhanced structural stability in B-doped configurations compared to Be-doped systems, with B-single-doped configurations showing the highest bond population and shortest average bond length. The electronic properties revealed that increasing B-doping concentrations led to higher band gaps: B-single (0.191 eV), B-dual (0.387 eV) and B-tri (0.44 eV). In contrast, the Be-doped configuration exhibited higher band gaps that decreased with increasing doping: Be-single (0.60 eV), Be-dual (0.550 eV), and Be-tri-doped (0.420 eV), suggesting potential for enhanced carrier mobility. The optical analysis revealed redshifted absorption peaks for B-single-doped graphene, suitable for infrared optoelectronics, while higher B-doping concentrations induced blueshifts, enabling visible and UV applications. The Be-single doped displayed blue shifted peaks, while the Be-dual doped exhibited visible light absorption and the Be-tri-doped had extended absorption peaks in the infrared region, making them suitable for UV applications, and IR image sensors. Additionally, Be-tri-doped graphene exhibited a high potential for photovoltaics, displaying multiple peaks in the visible range (1.6-2.4 eV), thus providing broader absorption properties. These findings provide valuable insight for tailoring the properties of graphene through controlled B and Be doping for diverse optoelectronic applications. The study demonstrates that Be and B doping can induce band gaps in graphene up to 0.60 eV and 0.44 eV, respectively, meeting the requirements for graphene based ON/OFF transistors. Future research can explore modelling graphene-based heterostructures for next-generation optoelectronics, leveraging their high charge mobilities and tuneable band structures.

CHAPTER 1 : INTRODUCTION

1.1 Research Background

Rapid economic and demographic growth has increased energy demand globally, and fossil fuels account for a significant portion of electricity generation. Therefore, a switch to renewables is imperative due to the rapid depletion of polluting energy sources (Ishaq et al., 2022). Moreover, the emissions of carbon dioxide from fossil fuels have contributed to the greenhouse effect, resulting in dire environmental consequences (Hu et al., 2022). Solar power stands out as the most reliable and appealing sustainable energy option for achieving energy security due to its abundance, environmental and socioeconomic benefits (Nashed et al., 2013; Mehmood et al., 2015; X. Chen et al., 2022).

Moreover, graphene has continued to receive significant research interest as a valuable material for photovoltaic and optoelectronic applications due to its tremendous potential (Gulati et al., 2022). The applications range from bulk materials to molecular-level structures because of the exceptional properties of graphene (Smarhak & Voves, 2022). It is a one-atom-thick two-dimensional sp^2 hexagonal lattice with its two carbon atoms at non-equivalent positions forming two interpenetrating triangular sublattices X and Ψ (Mhamdi et al., 2022; Nandee et al., 2022). The two non-equivalent sites are identified by χ and Ψ where $\vec{\chi}$ and $\vec{\psi}$ represent the fundamental unit vectors as indicated in Figure 1.1. Its exceptional properties have accelerated great research interest in optoelectronic devices due to its potential to replace silicon and indium tin oxide in flexible ultrathin solar cells (Kladkaew et al., 2022).

Furthermore, it is an excellent electron transport material that can enhance the mobility of carrier concentrations in composite structures. The high electron mobility in graphene helps to facilitate the isolation of the photoexcited electron-hole pairs. Thus, it has excellent electrical conductivities and optical properties, which are determined by the band structure and its atomic geometry, giving a theoretical explanation of the excellent performance of graphene in optoelectronics and sensing devices (Gong, Feng, et al., 2022; Gong, Shen, et al., 2022). In addition, graphene has been widely used in dye-sensitised solar cells (DSSCs), with promising results showing that they can improve light harvesting efficiency and charge transfer qualities. (Y. Li et al., 2019).

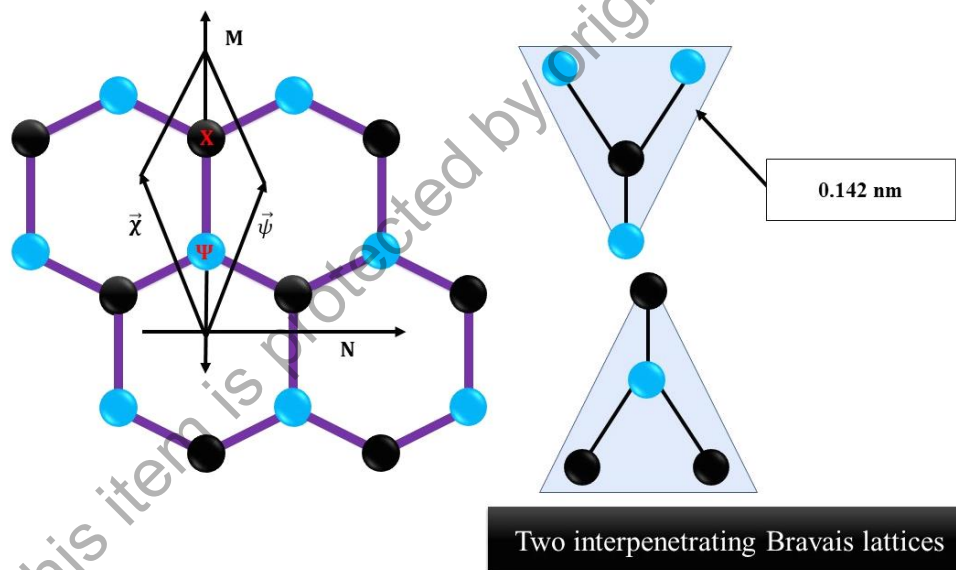


Figure 1.1 The schematic illustration shows the two carbon atoms in the unit cells of graphene with its Bravais lattices, and the primitive vectors

Meanwhile, a few of the approaches explored in the literature to study the properties of graphene include stacking configuration (Shu et al., 2022), mechanical strain (Movaghgharnezhad et al., 2023), chemical functionalisation (Carrasco et al., 2023), and heteroatom doping (Olatomiwa et al., 2023). Among these approaches, heteroatom doping is the most promising for modifying graphene's electrical, transport,

and optical characteristics(Olaniyan & Pretoria, 2018). Moreover, several studies show that nitrogen (N) and boron (B) are extensively explored in the literature due to their proximity to carbon atoms(Srivastava et al., 2019; Yutomo et al., 2021). Despite being the natural alternatives for graphene carbon atoms, other atomic elements such as Beryllium (Be), iron (Fe), and sulphur are being studied to alter the properties of graphene (Gharib & Arab, 2023; Olaniyan et al., 2018). This is sufficiently discussed in Section 2.6 of the next chapter.

Therefore, this study employs the first principles framework to model the electronic and optical properties of pure and modelled B and Be-doped graphene systems for designing efficient, low-cost, and environmentally friendly solar cells with optimal absorption. Therefore, these findings will serve as a new benchmark for future theoretical studies.

1.2 Problem Statement

The switch to solar power has accelerated lately due to its potential to provide reliable, affordable, and sustainable energy for all. However, conventional photovoltaic materials such as Indium tin oxide (ITO) employed as electrode materials are hard and brittle with poor mechanical properties and are relatively expensive (S. Chen et al., 2022; Miao & Fan, 2023).

Graphene has emerged as a promising alternative to ITO. It has lower sheet resistance due to its high electron mobility (S. Chen et al., 2022; Renuka et al., 2022). Moreover, graphene has exceptional mechanical strength, conductivity, and optical

transparency, surpassing other carbon-based materials such as Carbon nanotubes (CNTs). Specifically, graphene's planar structure, remarkable carrier mobility ranging from $\sim 100,000 \text{ cm}^2\text{V}^{-1}\text{S}^{-1}$ to $230,000 \text{ cm}^2\text{V}^{-1}\text{S}^{-1}$ in suspended structures outperform the carrier mobility of up to $\sim 80,000 \text{ cm}^2 \text{V}^{-1}\text{S}^{-1}$ in semiconducting single-walled CNTs. Additionally, graphene's high optical transparency of approximately 97% further distinguishes it from CNTs making it a suitable material for transparent conductive films. Thus, the superior geometry, carrier mobility and optical properties of graphene highlights its potential for highly efficient graphene-based optoelectronics and wearable devices.

Despite these superlatives, challenges persist in exploiting graphene's potential, especially its behaviour at the atomic level, semi-metallic nature, and lack of intrinsic band gap. This lack of band gap is due to the maximum valence band and minimum conduction band meeting at the k point in the Brillouin zone, forming the Dirac point. Moreover, it is difficult to induce a band gap in graphene due to the three discrete symmetries protected by the degeneracy at the Dirac point: the time reversal, inversion, and rotation by 120° (Bora et al., 2022; Prabhakar & Melnik, 2022; Yari et al., 2022). Thus, breaking these symmetries is essential for opening a band gap, but challenging to achieve without greatly altering graphene's electronic properties. This behaviour highlights the key difference between conventional semiconducting materials such as silicon that rely on band gaps to control the electron flow, an attribute absent in graphene (Bora et al., 2022; Kolář et al., 2022; Smith et al., 2019). This limitation poses a great challenge to its integration into semiconducting devices.

Additionally, there is an insufficient understanding of the underlying principles that govern the doping of graphene, as well as how dopant atoms affect the optical properties of graphene for photovoltaic and optoelectronics in the electromagnetic spectrum (Abdullah et al., 2020; Dobrota et al., 2022; Lv & Terrones, 2012). Moreover, the obtained results of substitutional doping of graphene are plagued with discrepancies due to the choice of the exchange-correlation (XC) functional, the basis set, and the wrong input parameters (Olatomiwa et al., 2023).

Furthermore, photovoltaics has poor conversion efficiency and may not be able to replace fossil fuels or have a significant impact on energy generation if these issues are not fully addressed (Prabhakar & Melnik, 2022). Its overall efficiencies are still very low, which can be associated with limitations in optical losses such as partial absorption and the high surface reflectivity of crystalline silicon (14.78%) (D. Zhang et al., 2022). Therefore, the shortcomings in this solar cell material necessitate the importance of modelling the optoelectronic properties of graphene at the atomic level to determine their best absorption sites (Y. Chen et al., 2022; Perrakis et al., 2020; Zhao et al., 2020).

1.3 Objectives of the Research

This work investigated the structural, electronic, and optical properties of pure graphene and Boron- and Beryllium-doped graphene using the density functional theory approach for potential applications in photovoltaics and optoelectronics. The following objectives were carried out to achieve this aim:

- i To investigate the structural, electronic, and optical properties of pure graphene using the CASTEP code.
- ii To investigate the structural, electronic, and optical properties of Boron and Beryllium doped graphene using the CASTEP code.
- iii To identify the best electronic, and optical properties from Boron and Beryllium doped graphene models from the CASTEP code.

1.4 Research Scope

The following scopes were carried out to fulfil the goals.

- i The atomic structure of pure graphene was generated in CASTEP after extracting the crystallographic information file (cif) from the materials project to file.cell and the structure was visualised using VESTA. A $4 \times 4 \times 1$ (32 carbon atoms) graphene supercell was generated. The parameter optimisation was performed to determine the plane wave cutoff energy and the k-point. Furthermore, pure graphene's relaxed state was determined by geometry optimisation. The band structures were calculated using GGA-PBE pseudopotential. Pure graphene's density of state (DOS) was determined to characterise its electronic properties. Lastly, the optical properties of pristine graphene were calculated.
- ii The graphene supercell was doped at different atomic positions and percentages with boron and beryllium atoms. The optimised atomic positions of graphene supercells were determined by performing geometry

optimisation. The electronic properties (band structure, density of states), and the optical properties were evaluated using CASTEP.

- iii The influence of the boron and beryllium dopants on the dielectric properties of graphene was determined for photovoltaic and optoelectronic applications.

1.5 Limitations

In this study, here is a list of the limitations faced in modelling the structural, electronic, and optical properties of graphene using density functional theory.

- i Access to high-performance computing clusters and supercomputers.
- ii long simulation time, which is a result of the computing resources used for my calculations.
- iii The inability to model co-doped graphene systems with larger cells.
- iv The cost of accessing the computing resources needed to model properties of graphene.

CHAPTER 2 : LITERATURE REVIEW

2.1 Introduction

This chapter is composed of two distinct parts. The first section provides an overview of specified properties of pristine and doped graphene, as well as related topics, based on the title of our study. The historical background of graphene is presented in Section 2.2. Meanwhile, in sections (2.3, 2.4, and 2.5) the structural, electronic, and optical properties of pure graphene are discussed. Furthermore, the modification of the electronic and optical properties of graphene via substitutional doping was presented.

The second part also gives an overview of the different density functional theory models employed in modelling the properties of the graphene material. Moreover, the foundations of density functional theory are briefly described, starting with the formulation of the Schrodinger equation and the Hartree-Fock, Hohenberg, Kohn, and Sham theorems in subsections 2.7.1 to 2.7.5.

Finally, the exchange-correlation functionals such as the local density approximation, generalised gradient approximation, and hybrid functional are briefly discussed in Sections 2.7.6 to 2.7.9, respectively. The linearised plane wave was briefly explored in Section 2.7.10. A brief discussion on the CASTEP code employed in this study concludes this review.